HHS Public Access

Author manuscript

J Immunol. Author manuscript; available in PMC 2019 July 15.

Published in final edited form as:

J Immunol. 2019 January 15; 202(2): 527–538. doi:10.4049/jimmunol.1700783.

G2A Protects Mice against Sepsis by Modulating Kupffer Cell Activation: Cooperativity with Adenosine Receptor 2b

Hong-Mei Li[#*], **Ji Hye Jang**[#*], **Jun-Sub Jung**[#*], **Jiseon Shin**[#*], **Chul O. Park**[†], **Yeon-Ja Kim**[*], **Won-Gyun Ahn**[*], **Ju-Suk Nam**[*], **Chang-Won Hong**[*,2], **Jongho Lee**[*], **Yu-Jin Jung**[‡], **Jiang-Fan Chen**[§], **Katya Ravid**[¶], **H. Thomas Lee**[‖], **Won-Ki Huh**[†], **Janusz H. Kabarowski**[#], and **Dong-Keun Song**[*]

[*]Department of Pharmacology, Institute of Natural Medicine, College of Medicine, Hallym University, Chuncheon, Gangwon-do 24252, Republic of Korea

[†]Department of Biological Sciences, Seoul National University, Gwanak-ro, Gwanak-gu, Seoul 08826, Korea

[‡]Department of Biological Sciences, Kangwon National University, Chuncheon, Gangwon-do 24341, Republic of Korea

[§]Department of Neurology, Boston University School of Medicine, Boston, MA 02118

[¶]Departments of Medicine and Biochemistry, Boston University School of Medicine, Boston, MA 02118

[‖]Department of Anesthesiology, College of Physicians and Surgeons of Columbia University, New York, NY 10032

[#]Department of Microbiology, University of Alabama at Birmingham, Birmingham, AL 35294

[#] These authors contributed equally to this work.

Abstract

G2A is a GPCR abundantly expressed in immune cells. G2A$^{-/-}$ mice showed higher lethality, higher plasma cytokines, and an impaired bacterial clearance in response to a murine model of sepsis (cecal ligation and puncture), which were blocked by $GdCl_3$, an inhibitor of Kupffer cells. Anti-IL-10 Ab reversed the impaired bacterial clearance in G2A$^{-/-}$ mice. Indomethacin effectively blocked both the increased i.p. IL-10 levels and the impaired bacterial clearance, indicating that disturbed PG system is the proximal cause of these phenomena. Stimulation with LPS/C5a induced an increase in *Escherichia coli* phagocytosis and intracellular cAMP levels in G2A$^{+/+}$ peritoneal macrophages but not G2A$^{-/-}$ cells, which showed more PGE_2/nitrite release and intracellular reactive oxygen species levels. Heterologous coexpression of G2A and adenosine receptor type 2b (A2bAR) induced a synergistic increase in cAMP signaling in a ligand-

Address correspondence and reprint request to Dr. Dong-Keun Song, Department of Pharmacology, Institute of Natural Medicine, College of Medicine, Hallym University, Chuncheon, Gangwon-do 24252, Republic of Korea. dksong@hallym.ac.kr.

[2]Current address: Department of Physiology, College of Medicine, Kyungpook National University, Daegu, Republic of Korea.

Disclosures

The authors have no financial conflicts of interest.

The online version of this article contains supplemental material.

independent manner, with the evidence of physical interaction of G2A with A2bAR. BAY 60–6583, a specific agonist for A2bAR, increased intracellular cAMP levels in Kupffer cells from $G2A^{+/+}$ but not from $G2A^{-/-}$ mice. Both G2A and A2bAR were required for antiseptic action of lysophosphatidylcholine. These results show inappropriate activation of $G2A^{-/-}$ Kupffer cells to septic insults due to an impaired cAMP signaling possibly by lack of interaction with A2bAR.

Sepsis remains a serious threat to human health, accounting for more than 250,000 deaths per year for the US alone (1), with no current specific therapeutic agent. For the development of therapeutic strategy for sepsis, the understanding of the pathophysiology of sepsis needs to be improved.

G2A (from G2 accumulation) is a G protein-coupled receptor (GPCR) abundantly expressed in various innate and adaptive immune cells (2). G2A has been shown to couple with multiple G proteins, including $G\alpha_s$, $G\alpha_q$, and $G\alpha_{13}$ (3). $G2A^{-/-}$ mice were shown to have abnormal expansion of B and T cell population and to develop a late-onset autoimmune disease w(4). Double knockout mice of $G2A^{-/-}$/low-density lipoprotein receptor ($LDLR^{-/-}$) and $G2A^{-/-}$/$ApoE^{-/-}$ were shown to promote macrophages accumulation/activation in atherosclerotic lesions (5, 6). However, the mechanisms of $G2A^{-/-}$ cells to show altered inflammatory signaling have not been fully addressed. Further, the response of $G2A^{-/-}$ mice to septic insults has not yet been studied.

Lysophosphatidylcholine (LPC), an endogenous immune modulator (7), is regarded as a G2A activator (8), as many actions of LPC depends on G2A (9–12). Previously, we reported that LPC has a protective effect against a murine model of sepsis (cecal ligation and puncture [CLP]), which was blocked by administration of anti-G2A Ab, suggesting the involvement of G2A in the antiseptic action of LPC (13). In the subsequent experiment, interestingly, we observed that $G2A^{-/-}$ mice had a higher lethality in CLP. Thus, we set out to study the mechanisms for the increased CLP lethality in $G2A^{-/-}$ mice.

We found that absence of G2A induces aberrant activations of Kupffer cells and peritoneal macrophages in response to septic insults (both in vivo and in vitro), resulting in impaired bacterial clearance due to disturbed PG systems. Furthermore, absence of G2A induced an impaired cAMP signaling, possibly due to lack of positive interaction with adenosine receptor A2b (A2bAR).

Materials and Methods

Mice

Six- to eight-week-old male C57BL/6J and $G2A^{-/-}$ (B6 background) mice were used in this study. The experiments were approved by the Experimentation Committee (Hallym University). All the mice were housed under specific pathogen-free conditions.

Sepsis models

CLP was performed as described previously (13). Mice were anesthetized with 50 mg/kg pentobarbital i.p., a small abdominal midline incision was made, and the cecum was exposed. The cecum was mobilized and ligated below the ileocecal valve, punctured through

both surfaces once with a 22-gauge needle, and the abdomen was closed (13). For another sepsis model, 5×10^8 *Escherichia coli* was i.p. injected to induce bacterial peritonitis. Survival was monitored once daily for 10 d.

Splenectomy

Splenectomy was performed under deep anesthesia using pentobarbital (50 mg/kg, i.p.). A left-sided infracostal 0.5-cm incision was made, the peritoneum was opened, and the splenic artery and vein were ligated with sterilized 4–0 silk sutures separately. Spleen was removed, and the incised abdominal muscles and skin were closed using sterilized 4–0 silk sutures (14).

In vivo macrophage inhibition or depletion

Kupffer cells were inhibited or depleted using gadolinium chloride ($GdCl_3$) (20 mg/kg; Sigma-Aldrich) administered via tail vein 24 h before *E. coli* injection or CLP. Control mice were treated with equivalent volume of saline injection.

Determination of bacterial burden

For determination of bacterial burden in vivo, mice were anesthetized at 24 h after CLP or 16 h after *E. coli* injection. Peritoneal lavage fluid was collected aseptically and diluted in sterile PBS, plated onto Lysogeny broth agar plates, incubated overnight at 37°C, and the numbers of CFUs were counted.

Determination of phagocytosis and bacterial killing

Bactericidal activity was determined as described previously (13, 15). Thioglycolate-induced macrophages (1×10^6/ml) were seeded on a 24-well plate in a humidified incubator (37°C, 5% CO_2). Macrophages were then incubated with 10^7 *E. coli* (macrophage: *E. coli* = 1:10) for 30 min. After 30 min of incubation for the uptake of *E. coli*, unengulfed *E. coli* were washed out twice with PBS containing gentamicin (12.5 μg/ml) and another twice with PBS. For determination of phagocytosed *E. coli* number, the plate was lysed with 0.1% Triton X-100 in PBS after 30 min of *E. coli* uptake. Then, *E. coli* were plated onto Lysogeny broth agar plates, incubated overnight at 37°C, and the numbers of CFUs were counted. For measurement of bactericidal activity, cells were incubated for 2 h after 30-min incubation for bacterial uptake. The percentage of killing was calculated as 100 × (1—CFUs after 2-h incubation/CFUs before 30-min incubation). For determination of the effects of C5a (Sino Biological), LPS (Sigma-Aldrich), or C5a/LPS, macrophages were incubated with each stimulator for 5 h, and then phagocytosis assay was performed. For the determination of the effects of inhibitors, protein kinase A (PKA) inhibitor (H-89, 10 mM; Tocris Bio-science), exchange protein directly activated by cAMP (EPAC) inhibitor (ESI-09, 10 μM; Tocris Bioscience), or mTOR inhibitor (rapamycin, 100 nM; Sigma-Aldrich) were applied before the addition of C5a/LPS.

Isolation of Kupffer cells

Kupffer cells were isolated from mice liver. In brief, under deep anesthesia using pentobarbital (50 mg/kg, i.p.), the liver was perfused in situ with 10 ml of PBS (37°C) in the

nonrecirculating fashion to drive out RBCs and subsequently perfused with 10 ml of RPMI 1640 (Hyclone) containing 0.1% collagenase (type IV; Sigma-Aldrich). The liver was removed, minced, and filtered through the mesh. The samples were suspended in RPMI 1640 and centrifuged at 300 × *g* for 5 min at 4°C; the cell sediments were resuspended with RPMI 1640 and centrifuged at 50 × *g* for 1 min. The top aqueous phase containing mainly nonparenchymal cells was reserved. To further purify the cells, cells were seeded on the culture plate and incubated for 2–3 h in a humidified incubator (37°C, 5% CO_2). Nonadherent cells were removed from the dish by washing with PBS, and the adherent cells were Kupffer cells (16). For the experiment with BAY 60–6583 (Tocris Bioscience), the isolated Kupffer cells from $G2A^{+/+}$ and $G2A^{-/-}$mice were preincubated with LPS (1 μg/ml) for 24 h, and then LPS was washed out, and the cells were exposed to BAY 60–6583 (1 μM) for 10 min, and the intracellular cAMP levels were measured.

Assay of cytokines and other mediators

Plasma cytokines were measured for MCP-1, TNF-α, IL-6, and IL-10 using a Cytometric Bead Array according to manufacturer's instructions (BD Biosciences). Adenosine was measured using HPLC with fluorescence detection (excitation: 280 nm, emission: 380 nm) (17). Mobile phase consisted of 12% methanol and 88% 10mM KH_2PO_4 (pH = 3.5); flow rate was 0.9 ml/min. Levels of prostaglandin D_2 (PGD_2; Cusabio Biotech), PGE_2 (Cayman), cAMP (Enzo Life Sciences), IL-6, IL-10 (BioLegend), TNF-α (AbFrontier), IL-1β (eBioscience), high mobility group box 1 (HMGB1) (IBL international), and lactate dehydrogenase (LDH) (Takara) were determined using ELISA kits. Nitrate levels in the medium were determined using Griess reagent.

Cell culture

Mice were injected with 1 ml of 3% thioglycolate medium into peritoneum. Four days later, cells were collected by injecting sterile ice-cold PBS into the peritoneal cavity and plated in RPMI supplemented with 10% FBS, 100 U of penicillin, and 100 μg/ml streptomycin. Macrophages were incubated overnight (37°C, 5% CO_2) and washed with fresh medium to remove nonadherent cells. G2A-transfected HEK-293 cells were cultured in DMEM supplemented with 10% FBS, 100 U of penicillin, and 100 μg/ml streptomycin at humidified incubator (37°C, 5% CO_2).

Western blot

Kupffer cells and thioglycolate-induced macrophages were lysed in RIPA buffer containing protease inhibitor and phosphatase inhibitor for 30 min on ice. After that, protein concentrations were determined using a Bio-Rad colorimetric protein assay kit. Proteins were separated on SDS-PAGE gels and transferred onto a nitrocellulose membrane. Caspase-1 (eBio-science), Akt, mTOR, p70S6K, EKR, p38, Ikb-α (Cell Signaling Technology), COX-2 (Cayman), β-actin (Santa Cruz Biotechnology) were used as the primary Abs. The membrane was then incubated with the corresponding anti-mouse and anti-rabbit HRP-conjugated secondary Ab. Proteins were detected using the ECL system.

Flow cytometry

To determine the expression of Ly6G, CD11b, and F4/80, cells were isolated from peritoneal lavage fluid at 24 h post-CLP and fixed with Cytofix for 30 min in 4°C. After washing, cells were stained with various Abs for 30 min in 4°C and assayed by using a flow cytometer (FACS Calibur). Data were analyzed by FlowJo software.

Real-time PCR

Total RNA from thioglycolate-induced macrophages was obtained by TRIzol method. cDNA was generated with ReverTra Ace qPCR RT Master Mix with gDNA Remover (Toyobo). mRNAs for G2A and A2b were quantified by Thunderbird SYBR qPCR Mix (Toyobo) using the Rotor-Gene Real-Time PCR System (QIAGEN). Results were evaluated by applying the cycle threshold (ACt) method and normalized to GAPDH.

Luciferase reporter assay

HEK-293 cells were cultured in DMEM supplemented with 10% FBS in a humidified incubator (37°C, 5% CO_2). Cells were transfected at 60–70% confluency in 48-well plates for 24 h using X-tremeGENE HP DNA Transfection Reagent kit (Roche) according to the manufacturer's instructions. Cells were transfected with G2A, A2bAR, or G2A + A2bAR, and cAMP luciferase reporter construct (Promega). Then, luciferase activity was evaluated with luminometer (Glomax, Promega, Sunnyvale, CA) using a Bright-Glo Luciferase Assay System (Promega) according to the manufacturer's recommendations.

Bimolecular fluorescence complementation analysis of G2A–A2bAR interaction

Cos-7 cells were seeded at a density of 7×10^3 cells per well in a black 96-well clear-bottom plate in 100 μl of DMEM supplemented with 10% FBS. G2A and A2bAR tagged with the N-terminal fragment of Venus and C-terminal fragment of Venus, respectively, were cloned into pcDNA3.1 vector (Invitrogen) and transfected into cells using Lipofectamine 2000 (Invitrogen) according to the manufacturer's protocol. At 48 h after transfection, cells were fixed with 2% formaldehyde and stained with Hoechst 33342 (Invitrogen). Bimolecular fluorescence complementation (BiFC) and nuclear images were captured using IN Cell Analyzer 2000 (GE Healthcare) using 20 × objective and 350/455 nm (for Hoechst) and 500/535 nm (for BiFC) excitation/emission filters with a polychroic mirror (QUAD2).

Statistical analysis

GraphPad Prism 5 software was used for statistical analysis of the data. Survival curves were analyzed by the log-rank test. Other data were analyzed by either one-way ANOVA followed by Bonferroni test or Student *t* test. All data were presented as mean ± SEM. For all analyses, $p < 0.05$ was considered statistically significant.

Results

G2A$^{-/-}$ mice show higher lethality in sepsis with changes, suggesting inappropriate activation of Kupffer cells

About 80% G2A$^{+/+}$ mice survived up to 10 d after CLP (one-puncture model) (Fig. 1A). Conversely, all the G2A$^{-/-}$ mice died by 8 d after CLP (Fig. 1A), demonstrating a markedly higher susceptibility to experimental sepsis. In the more severe (i.e., two-puncture CLP model) G2A$^{-/-}$ mice still tended to show the higher lethality; however, it did not reach statistical significance ($p = 0.13$) (Supplemental Fig. 1A).

Next, we compared the plasma cytokines levels in the G2A$^{+/+}$ and G2A$^{-/-}$ mice at 8 h post-CLP. As shown in Fig. 1B, the plasma levels of IL-6, IL-10, and TNF-α were markedly higher in the G2A$^{-/-}$ mice than those of G2A$^{+/+}$ mice. When HMGB1, a late mediator of sepsis (18), was measured at 24 h after CLP, G2A$^{-/-}$ mice also showed a significantly higher level of plasma HMGB1 (Fig. 1C).

Spleen and liver play important roles in pathogenesis of sepsis (19). Therefore, we examined whether spleen is responsible for the higher susceptibility of G2A$^{-/-}$ mice to CLP. After splenectomy, G2A$^{-/-}$ mice still had a higher susceptibility to sepsis than G2A$^{+/+}$ mice, indicating that spleen is not the responsible organ (Supplemental Fig. 1B).

Another important organ for innate immunity during sepsis is liver (20). As Kupffer cells are the major source for plasma levels of IL-6 (21) and IL-10 (22) during early (i.e., 3–12 h) post-CLP period, our results (Fig. 1B) suggest that Kupffer cells are overly activated in G2A$^{-/-}$ mice after CLP.

LPS administration induces a prompt PG D_2 release from Kupffer cells in the liver (23), which leads to an increased glucose output from the nearby hepatocytes via enhanced glycogenolysis (LPS → Kupffer cells → PGD_2 → hepatocyte glycogenolysis), ultimately resulting in hepatic glycogen depletion and transient hyperglycemia (24). Thus, we assessed PGD_2 level in the liver after CLP. As shown in Fig. 1D, PGD_2 level was significantly higher at 1 h in G2A$^{-/-}$ mice than in G2A$^{+/+}$ mice; however, at a later time point (i.e., 9 h), it tended to be lower ($p = 0.052$). At 3 h post-CLP, G2A$^{-/-}$ mice had hepatic glycogen more depleted than G2A$^{+/+}$ mice (Fig. 1E) and accompanying transient hyperglycemia (Fig. 1F). Taken together, these findings suggest that Kupffer cells are inappropriately activated in G2A$^{-/-}$ mice after CLP.

Kupffer cell inhibition blocks the enhanced susceptibility of G2A$^{-/-}$ mice to sepsis

$GdCl_3$ depletes or inhibits Kupffer cells (25). Thus, we examined whether pretreatment with $GdCl_3$ blocks the enhanced CLP lethality accompanied with various exaggerated changes observed in the G2A$^{-/-}$ mice (Fig. 1). $GdCl_3$ pretreatment (20 mg/kg, i.v.) did not affect CLP lethality in G2A$^{+/+}$ mice (Fig. 2A). However, strikingly, $GdCl_3$ markedly rescued G2A$^{-/-}$ mice from CLP lethality (Fig. 2A), resulting in no significant difference in CLP lethality between G2A$^{+/+}$ and G2A$^{-/-}$ mice. Similar findings of $GdCl_3$ pretreatment were also observed in sepsis induced by *E. coli* infection in G2A$^{-/-}$ mice (Fig. 2B).

$G2A^{-/-}$ mice showed a significantly lower rectal temperature (one of the in vivo parameters for the severity of sepsis) than $G2A^{+/+}$ mice at 24 h after CLP surgery, but the difference was eliminated with $GdCl_3$ pretreatment (Fig. 2C). All these results suggest that the higher CLP lethality in the $G2A^{-/-}$ mice (Fig. 1A) is due to inappropriate activation of Kupffer cells.

HMGB1 is released from activated macrophages via inflammasome NLRP3 along with IL-1β and LDH (26). As shown in Fig. 2D, the plasma levels of HMGB1, IL-1β, and LDH were significantly higher in $G2A^{-/-}$ mice at 24 h post-CLP compared with $G2A^{+/+}$ mice. For HMGB1, the difference between $G2A^{+/+}$ and $G2A^{-/-}$ mice disappeared by $GdCl_3$ pretreatment. Post-CLP IL-1b and LDH levels in G2A $^{/}$ mice were significantly lessened by $GdCl_3$ pretreatment. Next, we directly tested inflamma- some NLRP3 activity in the Kupffer cells isolated from $G2A^{+/+}$ and $G2A^{-/-}$ mice. Kupffer cells isolated from $G2A^{-/-}$, not G2A $^{+/+}$, mice showed an increased cytotoxicity (Fig. 2E) and more active caspase-1 (Supplemental Fig. 1C) in response to monosodium urate (MSU, 200 μg/ml) and ATP (5 mM). Furthermore, $GdCl_3$ pretreatment eliminated or alleviated the difference between G2A $^{+/+}$ and $G2A^{-/-}$ mice in plasma IL-6, IL-10, and TNF-α levels (Fig. 2F).

Next, we directly measured IL-1β and IL-10 released from isolated Kupffer cells from G2A $^{+/+}$ and $G2A^{-/-}$ mice. Both basal and LPS-stimulated release of IL-1β (Supplemental Fig. 1D) and IL-10 (Fig. 2G) were significantly more marked in $G2A^{-/-}$ Kupffer cells compared with $G2A^{+/+}$ Kupffer cells. Taken together, these results show that inappropriate activation of $G2A^{-/-}$ Kupffer cells in response to septic insults leads to the higher susceptibility of $G2A^{-/-}$ mice to sepsis.

Impaired bacterial clearance in $G2A^{-/-}$ mice is rescued by pretreatment with $GdCl_3$ or anti—IL-10 Ab

Sepsis is frequently accompanied with immunosuppression as manifested by impaired bacterial clearance (27). To determine whether G2A affects bacterial clearance in CLP- and *E. coli-in-* duced peritonitis, we evaluated the number of viable bacteria in peritoneal lavage fluid from $G2A^{+/+}$ and $G2A^{-/-}$ mice at 19–24 h post-CLP or 18 h postinoculation of *E. coli* (Fig. 3A). $G2A^{-/-}$ mice had an impaired bacterial clearance as shown by a significantly higher number of viable bacteria in peritoneal cavity compared with $G2A^{+/+}$ mice (Fig. 3A). Impaired bacterial clearance can be resulted from impaired immune cell infiltration into the peritoneal cavity. However, there was no difference between $G2A^{+/+}$ and $G2A^{-/-}$ mice in the peritoneal infiltration of macrophages and neutrophils (Supplemental Fig. 2A–C).

Next, we evaluated the intracellular number of bacteria in peritoneal exudate cells at 17 h after *E. coli* infection. $G2A^{-/-}$ mice had significantly fewer intracellular numbers of bacteria in peritoneal exudate cells compared with $G2A^{+/+}$ mice, implying impaired phagocytosis ability (Fig. 3B, left panel). However, isolated peritoneal exudate cells as well as Kupffer cells and bone marrow-derived macrophages from $G2A^{+/+}$ and $G2A^{-/-}$ cells had similar phagocytosis ability when measured in in vitro condition (Supplemental Fig. 2D–F).

Thus, we hypothesized that a humoral factor in the peritoneal cavity inhibits phagocytosis of peritoneal exudate cells in $G2A^{-/-}$ mice. IL-10 is known to inhibit phagocytosis (28). As plasma IL-10 level was markedly increased in $G2A^{-/-}$ mice (Figs. 1B, 2F), we hypothesized

that i.p. IL-10 level could also be increased in $G2A^{-/-}$` mice, leading to inhibition of phagocytosis of peritoneal exudate cells. Thus, we examined IL-10 levels in peritoneal lavage fluid at 17 h after *E. coli* infection. $G2A^{-/-}$ mice showed markedly higher IL-10 levels in peritoneal lavage fluid compared with $G2A^{+/+}$ mice (Fig. 3B, right panel).

Next, we examined whether neutralizing IL-10 with anti-IL-10 Ab rescues the impaired bacterial clearance in $G2A^{-/-}$ mice. The result shows that this was the case (Fig. 3C), indicating that the impaired i.p. bacterial clearance was due to the increased i.p. IL-10 levels. Taken together, these results suggest that G2A plays an important role in bacterial clearance via modulation of IL-10 levels.

Next, we examined whether $GdCl_3$ pretreatment restores the impaired bacterial clearance and the increased i.p. IL-10 levels in $G2A^{-/-}$ mice. $GdCl_3$ pretreatment markedly decreased the number of viable bacteria in peritoneal lavage fluid in $G2A^{-/-}$ mice, whereas it tended to increase it in $G2A^{+/+}$ mice, resulting in a reversed significant difference between $G2A^{+/+}$ and $G2A^{-/-}$ mice (Fig. 3D, left panel). The increased IL-10 level in peritoneal lavage fluid in $G2A^{-/-}$ mice was effectively lowered by $GdCl_3$ pretreatment (Fig. 3D, right panel). Taken together, these results suggest that inappropriately activated Kupffer cells overly produce IL-10, resulting in impaired bacterial clearance in $G2A^{-/-}$ mice.

Next, as PGE_2 induces IL-10 release in the macrophages (29), to examine whether the higher IL-10 levels in peritoneal lavage fluid from the $G2A^{-/-}$ mice is induced by PGE_2, we measured PGE_2 levels in the peritoneal lavage fluid. As shown in Fig. 3E, in an intriguing similarity to the PGD_2 levels in the liver shown in Fig. 1D, PGE_2 levels were significantly increased at the early time point (4 h); however, it was significantly decreased at the later time point (15 h).

Next, to examine the causal relationship between levels of PGE_2 and IL-10, we examined the effect of indomethacin (a cyclooxygenase inhibitor) treatment on the peritoneal lavage fluid IL-10 levels. Indomethacin (5 mg/kg, i.p.) was injected 1 h before *E. coli* injection. As shown in Fig. 3F, indomethacin treatment effectively blocked the increased IL-10 levels (left panel) and the impaired bacterial clearance (right panel) in the $G2A^{-/-}$ mice. Taken together, these results suggest that the overly produced PGE_2 in the early time point results in increased IL-10 levels, which subsequently induces impaired bacterial clearance in $G2A^{-/-}$ mice.

Abnormal responses of $G2A^{-/-}$ macrophages to the in vitro condition of sepsis

G2A is abundantly expressed in the macrophages (30). Thus, we examined whether G2A affects macrophage activation in vitro, using thioglycolate-induced peritoneal macrophages. To mimic septic conditions more relevantly, we stimulated thioglycolate-induced macrophages with C5a (1 μg/ml) and LPS (1 μg/ml), two important endogenous and exogenous mediators of sepsis, respectively (31), and monitored levels of PGE_2, nitrite in the medium, and intracellular levels of reactive oxygen species (ROS) and cAMP. As shown in Fig. 4A–C, C5a had no effect in levels of PGE_2, nitrite, and ROS. Conversely, LPS increased them, how-ever, with no difference between $G2A^{+/+}$ and $G2A^{-/-}$ macro-phages, except in the case of PGE_2, where $G2A^{-/-}$ macrophages released significantly more PGE_2.

Interestingly, C5a/LPS cotreatment induced a marked difference between G2A$^{+/+}$ and G2A$^{-/-}$ macrophages in the increase in the levels of PGE_2, nitrite, and intracellular ROS (Fig. 4A–C). Particularly, for nitrite, the addition of C5a to LPS significantly decreased nitrite levels in the G2A$^{+/+}$ macrophages; however, it significantly increased nitrite levels in the G2A$^{-/-}$ macrophages (Fig. 4B).

One of the intracellular signaling effectors of G2A is cAMP (3). Intracellular cAMP level is an important regulating factor for macrophage activation (32); particularly, high intracellular cAMP levels inhibit the synthesis/release of macrophage NO/nitrite (33) and ROS production (34). Thus, we hypothesized that G2A$^{-/-}$ macrophages may have an impaired ability for cAMP increase after C5a/LPS stimulation. Remarkably, C5a/LPS significantly increased intracellular cAMP levels in G2A$^{+/+}$, but not G2A$^{-/-}$, macrophages (Fig. 4D).

Taken together, we found an in vitro sepsis-like condition that can differentiate G2A$^{-/-}$ from G2A$^{+/+}$ macrophages (i.e., C5a/ LPS costimulation). In this condition, G2A$^{-/-}$ macrophages showed features of inappropriate activation with the impaired ability of increasing intracellular cAMP levels. These findings suggest that G2A is involved in elevating cAMP levels in macrophages in response to C5a/LPS.

C5a/LPS markedly increases phagocytosis in G2A$^{+/+}$, but not G2A$^{-/-}$, macrophages via cAMP signaling

Next, we assessed *E. coli* phagocytosis in the thioglycolate-induced macrophages from G2A$^{+/+}$ and G2A$^{-/-}$ mice at 5 h after C5a/LPS stimulation. In the vehicle-treated group, there was no difference in *E. coli* phagocytosis between G2A$^{+/+}$ and G2A$^{-/-}$ macrophages. However, C5a/LPS stimulation for 5 h induced a marked increase (1.9-fold) in phagocytosis in G2A$^{+/+}$, but not G2A$^{-/-}$, macrophages (Fig. 5A).

Next, we examined whether the increased phagocytosis in G2A$^{+/+}$ macrophages was dependent on the cAMP signaling pathway. We treated macrophages with inhibitors for PKA and EPAC, two direct effectors of cAMP. As shown in Fig. 5A, both PKA inhibitor (H-89; 10 μM) and EPAC inhibitor (ESI-09; 10 μM) effectively blocked the C5a/LPS stimulation-induced increase in phagocytosis in G2A$^{+/+}$ macrophages, with no effect on G2A$^{-/-}$ macrophages. The inhibitory effect of H-89 on phagocytosis in macrophages has been previously reported (35). These data suggest that PKA and EPAC are involved in C5a/LPS-induced increase in phagocytosis of G2A$^{+/+}$ macrophages.

Next, we examined bactericidal activity of G2A$^{+/+}$ and G2A$^{-/-}$ macrophages. Interestingly, in contrast to phagocytosis, bactericidal activity of G2A$^{-/-}$ macrophages was markedly depressed in the basal condition compared with G2A$^{-/-}$ macrophages (Fig. 5B). C5a/LPS stimulation induced a significant increase in bactericidal activity of G2A$^{+/+}$, but not G2A$^{-/-}$, macrophages (Fig. 5B).

G2A enhances A2bAR-mediated cAMP signaling: direct physical interaction with A2bAR

A2bAR is a representative immune regulatory GPCR coupled to cAMP signaling (36). Its expression is markedly induced in the activated macrophages (37). We assessed mRNA expression of G2A and A2bAR in LPS-stimulated thioglycolate-induced G2A$^{+/+}$

macrophages using real-time quantitative PCR. mRNA levels of G2A (Fig. 6A) and A2bAR (Fig. 6B) were markedly increased at 5 h after LPS stimulation by 3.5- and 127- fold, respectively, consistent with the previous reports (38).

Next, we evaluated the effect of G2A on the cAMP-dependent signaling activity. After HEK-293 cells were transfected with G2A + cAMP-luciferase reporter construct (luc), A2bAR + cAMP-luc, and G2A + A2bAR + cAMP-luc reporter plasmids, luciferase activity representing cAMP-dependent signaling activity was measured in the absence of specific ligands for each GPCR (Fig. 6C). Overexpression of G2A and A2bAR elevated cAMP reporter luciferase activity by 3- and 33-fold, respectively (Fig. 6C). Interestingly, coexpression of G2A and A2bAR induced a synergistic increase in luciferase activity (i.e., nearly 30% increase compared with A2bAR-only expression).

Next, we examined whether G2A and A2bAR physically interact with each other using BiFC assay. Cos-7 cells coexpressing N-terminal fragment of Venus-tagged G2A and C-terminal fragment of Venus-tagged A2bAR exhibited a clear BiFC signal (Fig. 6D), indicating the presence of direct physical interaction between G2A and A2bAR. Taken together, these data suggest that G2A can significantly enhance A2bAR-mediated cAMP signaling via direct interaction with A2bAR in a ligand-independent manner.

Because the enhanced susceptibility of $G2A^{-/-}$ mice to sepsis was due to the inappropriate activation of Kupffer cells in response to septic stimuli (Fig. 2), we examined the cooperativity between G2A and A2bAR in the isolated Kupffer cells. Remarkably, BAY- 60–6583, a specific agonist for A2bR, markedly increased intracellular cAMP levels in the isolated Kupffer cells from $G2A^{+/+}$, but not $G2A^{-/-}$ mice (Fig. 6E), suggesting the cooperativity between G2A and A2bAR.

Rapamycin blocks C5a/LPS-induced increase in phagocytosis of $G2A^{+/+}$ macrophages

Akt pathway has been shown to be a target of cAMP (39). To further elucidate the differences in molecular signaling between $G2A^{+/+}$ and $G2A^{-/-}$ macrophages, we examined the protein levels of p-Akt, p-mTOR, and p-p70S6K after C5a/LPS stimulation. As shown in Fig. 7A–D, C5a/LPS stimulation significantly decreased Akt phosphorylation at T308 (but not at S473) and markedly increased p-mTOR and p-p70S6K in $G2A^{+/+}$, but not $G2A^{-/-}$, macrophages. As mTOR regulates phagosome and vacuole fission (40), we examined whether rapamycin, an inhibitor of mTOR, can inhibit the C5a/LPS-induced increase in phagocytosis of $G2A^{+/+}$ macrophages. As shown in Fig. 7E, rapamycin (100 nM) effectively inhibited the C5a/LPS-induced increase in phagocytosis in $G2A^{+/+}$ macrophages, consistent with a previous study that showed that rapamycin inhibits phagocytosis in macrophages (41). These data suggest that p-mTOR signaling is involved in C5a/LPS stimulation-induced increase in phagocytosis in $G2A^{+/+}$ macrophages.

LPC has no protective effect on CLP-induced sepsis in either $G2A^{-/-}$ or $A2bAR^{-/-}$ mice and in $GdCl_3$-pretreated mice

We previously reported that LPC (an effector for G2A) protection against CLP-induced lethality is blocked by anti-G2A Ab (13). In this study, we tried to confirm the involvement of G2A in the antiseptic effects of LPC using $G2A^{+/+}$ and $G2A^{-/-}$ mice. Sub-cutaneous

administration of LPC (10 mg/kg, four times at 12-h interval beginning 2 h after CLP) significantly increased survival in CLP in $G2A^{+/+}$ mice (Fig. 8A), as reported previously (13), but not in $G2A^{-/-}$ mice (Fig. 8B). Next, based on our previous finding of interaction between G2A and A2bAR (Fig. 6C–E), we investigated whether A2bAR is also involved in the antiseptic effects of LPC. Remarkably, LPC protected $A1AR^{-/-}$, $A2aAR^{-/-}$, and $A3AR^{-/-}$ (Supplemental Fig. 3A-C) but not $A2bAR^{-/-}$ (Fig. 8C) mice from CLP-induced lethality. Intriguingly, a s.c. injection of LPC (10 mg/kg) induced a significant increase in plasma adenosine levels in $G2A^{+/+}$ but not in $G2A^{-/-}$ mice (Fig. 8D). These results suggest that the protective effect of LPC against CLP-induced lethality depends on G2A and A2bAR, further suggesting the interaction between G2A and A2bAR.

Previously, we reported that LPC administration inhibits experimental sepsis-induced increase in plasma IL-1β levels (7). As we found in the current study that indomethacin effectively blocked both the increased i.p. IL-10 levels and the impaired bacterial clearance observed in $G2A^{-/-}$ mice (Fig. 3F), we became interested in examining the effect of indomethacin on the LPC inhibition of plasma IL-1β increase. Indomethacin pretreatment blocked the LPC inhibition of plasma IL-1β increase in CLP mice (Supplemental Fig. 3D), suggesting the involvement of PG systems in the antiseptic mechanisms of LPC.

Next, we examined whether thioglycolate-induced $A2bAR^{-/-}$ macrophages show no increase in phagocytosis in response to C5a/ LPS stimulation as in the case with $G2A^{-/-}$ macrophages (Fig. 5A). As shown in Fig. 8E, C5a/LPS stimulation could not increase phagocytosis in $A2bAR^{-/-}$ macrophages. These results suggest that C5a/LPS-induced increase in phagocytosis of macrophages depends on G2A and A2bAR, giving other evidence suggesting the interaction between G2A and A2bAR.

Finally, we examined whether pretreatment with $GdCl_3$ blocks LPC's antiseptic effects in CLP model. As shown in Fig. 8F, $GdCl_3$ pretreatment completely blocked the protective effects of LPC against CLP lethality. This result suggests that the protective effect of LPC against CLP-induced lethality depends on intact Kupffer cells.

Discussion

Kupffer cells, comprising up to 80% of tissue-resident macrophages in the body, are critically involved in innate immunity processes by the phagocytosis of bacteria by secretion of proinflammatory and anti-inflammatory cytokines and by the recruitment of other immune cells to the liver (42). Activated Kupffer cells release inflammatory cytokines (43) and are also a major source of IL-10 during septic peritonitis (44).

We found in the current study the increased susceptibility of G2A KO mice to sepsis. Remarkably, nearly all the differences between $G2A^{+/+}$ and $G2A^{-/-}$ mice in response to septic insults were blocked or at least alleviated by pretreatment with $GdCl_3$, a well-known specific inhibitor of Kupffer cells (25, 45) (Fig. 2), implicating G2A as an important modulator of Kupffer cells activation in response to septic stimuli. In line with this contention, the antiseptic actions of LPC, an activator of G2A, was lost by pretreatment with $GdCl_3$ (Fig. 8F), implicating the Kupffer cells as the target for the antiseptic actions of LPC.

Immune suppression is regarded as an important pathogenetic factor for determination of outcome of septic patients. Importantly, $G2A^{-/-}$ mice showed defects in bacterial clearance in sepsis (Fig. 3A). $G2A^{-/-}$ septic mice had particularly higher IL-10 levels both in plasma (Fig. 1B, middle panel) and in peritoneal fluid (Fig. 3B, right panel), and remarkably, anti-IL-10 Ab pre-treatment clearly rescued the impaired bacterial clearance in $G2A^{-/-}$ septic mice (Fig. 3C), displaying the link between G2A and IL-10 in the septic condition.

An additional important finding was that $G2A^{-/-}$ septic mice had dysregulated PG responses to septic insults (Figs. 1D, 3E). Furthermore, indomethacin, an inhibitor of PG synthesis, effectively reversed both the increased IL-10 levels (Fig. 3F, left panel) and the impaired bacterial clearance (Fig. 3F, right panel) in $G2A^{-/-}$ septic mice, proposing PGs, an important immune-modulating mediator, as an additional component of dysregulated immune environments for $G2A^{-/-}$ septic mice (G2A → PGs → IL-10). Kupffer cells are known to be the main source for PGD_2 and PGE_2 (23, 46, 47), which play important roles in the modulation of the inflammatory response (48, 49).

Because G2A is abundantly expressed in the macrophages (30), and sepsis is a systemic disease, we extended our study to the peritoneal macrophages. We attempted to delineate the differences between $G2A^{+/+}$ and $G2A^{-/-}$ macrophages in activation in response to C5a/LPS stimulation. We found significant differences in nitrite (NO) and intracellular ROS production between $G2A^{+/+}$ and $G2A^{-/-}$ macrophages (Fig. 4A, 4B). It is interesting that the presence or absence of G2A did not affect LPS-induced effects both in in vivo (H.-M. Li, J.-S. Jung, and D.-K. Song, unpublished observations) and in vitro conditions (Fig. 4), implying that G2A does not affect LPS signaling. G2A only affected the macrophage responses to C5a/LPS costimulation. Considering that C5aR is one of the GPCRs abundantly expressed in macrophages (50), it would be possible that an interaction between G2A and C5aR might also occur. These in vitro results suggest that G2A is required for macrophages to increase phagocytosis and bactericidal activity in septic condition (i.e., C5a/LPS stimulation) on the one hand, and on the other hand, G2A is required for macrophages not to be inappropriately activated, for example, in terms of release of PGE_2 and nitrite and increase in intracellular ROS.

cAMP, an important intracellular second messenger, modulate macrophage function (51); it inhibits macrophage activation (32, 52), NLRP3 inflammasome activation (53, 54), and ROS production (34). In line with this contention, C5a/LPS-stimulated $G2A^{-/-}$ macrophages released significantly more nitrite (NO) and had higher intracellular ROS level accompanied with a significantly low cAMP level compared with $G2A^{+/+}$ macrophages (Fig. 4). Further, for the isolated Kupffer cells, stimulation with MSU and ATP after priming with LPS induced cytotoxicity in $G2A^{-/-}$ but not $G2A^{+/+}$ macrophages (Fig. 2E), in line with the previous reports on the negative regulation of NLRP3 inflamma-some activation by cAMP (53, 54).

A2bAR (via cAMP signaling), the expression of which is markedly induced by LPS (Fig. 6B), a typical septic stimulus (55), is one of the major GPCRs involved in immunomodulation (56). Particularly, A2bAR has many anti-inflammatory effects (57–59). In line with these reports, the protective effect of A2bAR against CLP was reported (60).

In the current study, a ligand-independent cooperativity between G2A and A2bAR in the cAMP signaling was observed (Fig. 6C) with evidence of the direct physical interaction between G2A and A2bAR in the heterologous overexpression systems (Fig. 6D). Furthermore, the cooperativity between G2A and A2bAR in the specific A2bAR agonist (BAY 60–6583)-induced cAMP signaling was also suggested in the isolated Kupffer cells (Fig. 6E). Similar experiments using G2A agonists are needed to further support the cooperativity between G2A and A2bAR in the cAMP signaling. Inhibition of A2aAR signaling by heteromer formation with A2bAR was recently reported (61). However, the evidence for the cooperative heteromer formation of A2bAR with other GPCRs has not been reported.

Additionally, the increased phagocytosis in $G2A^{+/+}$ macro-phages after C5a/LPS treatment was inhibited by H-89 and ESI-09 (Fig. 5A). In line with these data, defective phagocytosis from C3H/HeJ peritoneal macrophages was reported to be corrected by cAMP-elevating agents (62). Further, isoproterenol-induced increase in *E. coli* phagocytosis in macrophages was reported to be prevented by H-89 (35). As cAMP-elevating agents promote resolution of inflammation (63, 64) and induce macrophage polarization with a phenotype that enhances the resolution of systemic inflammation (65), the lower levels of cAMP in stimulated macrophages (Fig. 4D) may be linked to the more severe sepsis in $G2A^{-/-}$ mice (Fig. 1).

PI3K/Akt pathway is an important signaling pathway in in-flammatory cells (66). cAMP elevation induces Akt inhibition via PKA and EPAC (67, 68). Akt signaling was evaluated to understand the signaling downstream of cAMP in C5a/LPS-stimulated $G2A^{-/-}$ macrophages. Usually, Akt, mTOR, and p-p70S6K signaling change in the same direction. However, some reports show opposite changes between Akt and mTOR/p-p70S6K signaling (69–72). In line with the aforementioned studies, the data showed that a significant decrease in Akt (T308) phosphorylation accompanied a significant increase in p-mTOR and p-p70S6K in C5a/LPS-stimulated $G2A^{+/+}$, but not $G2A^{-/-}$, macrophages (Fig. 7A–D). It is well known that mTOR regulates phagosome, and rapamycin inhibits macrophage phagocytosis (40, 41, 73, 74). In line with this contention, the increased phagocytosis in C5a/ LPS-stimulated $G2A^{+/+}$ macrophages was effectively blocked by rapamycin (Fig. 7E), implicating the involvement of mTOR signaling.

Quite intriguingly, we found several additional pieces of experimental evidence for the intimate relationship between G2A and A2bAR in sepsis. Both G2A and A2bAR were required for the antiseptic actions of LPC (Fig. 8A–C) and for C5a/LPS costimulation-induced increase in phagocytosis in peritoneal macrophage (Fig. 8E). Additionally, for another line of evidence for G2A and A2bAR interaction, we observed that G2A is required for LPC administration-induced increase in plasma levels of adenosine, an endogenous agonist for A2bAR (Fig. 8D). Detailed mechanistic studies remain to be done to fully delineate the complex relationship among LPC, G2A, and A2bAR in the context of sepsis.

Collectively, our findings show the protective role of G2A during sepsis. It is suggested* that G2A in macrophages functions as a ballast point in the context of sepsis, helping macrophages to respond adequately but not inappropriately. G2A acts as a booster for cAMP signaling possibly by interaction with A2bAR, resulting in restraining of excessive

inflammatory responses and, at the same time, increasing phagocytosis. This action mechanism of G2A could shed light on the previously unexplained proin-flammatory characteristics of $G2A^{-/-}$ cells (5, 6, 75, 76) and make G2A act as a useful fine modulator for macrophage activation in the pathologic conditions of sepsis.

Supplementary Material

Refer to Web version on PubMed Central for supplementary material.

Acknowledgments

We appreciate the generous supply of $A1AR^{-/-}$ mice from Dr. Jurgen Schnermann (National Institute of Diabetes and Digestive and Kidney Diseases/National Institutes of Health, Bethesda, MD), $A3AR^{-/-}$ mice from Dr. Marlene Jacobson (Merck & Co., Whitehouse Station, NJ), and FLAG-tagged hG2A plasmid from Dr. Takao Shimizu (The Tokyo University).

This work was supported by grants from the National Research Foundation of Korea (NRF-2015R1D1A1A01058532 and NRF-2017R1D1A1B03035569 to D.-K.S.; 2015R1A2A1A01007871 to W.-K.H.).

Abbreviations used in this article:

A2bAR	adenosine receptor A2b
BiFC	bimolecular fluorescence complementation
CLP	cecal ligation and puncture
EPAC	exchange protein directly activated by cAMP
$GdCl_3$	gadolinium chloride
GPCR	G protein–coupled receptor
HMGB1	high mobility group box 1
LDH	lactate dehydrogenase
LPC	lysophosphatidylcholine
luc	luciferase reporter construct
PGD_2	prostaglandin D_2
PKA	protein kinase A
ROS	reactive oxygen species

References

1. Tidswell M, and LaRosa SP. 2011 Toll-like receptor-4 antagonist eritoran tetrasodium for severe sepsis. Expert Rev. Anti Infect. Ther. 9: 507–520. [PubMed: 21609262]
2. Ellison MA, Ambruso DR, and Silliman CC. 2012 Therapeutic options for transfusion related acute lung injury; the potential of the G2A receptor. Curr. Pharm. Des. 18: 3255–3259. [PubMed: 22621271]

3. Lin P, and Ye RD. 2003 The lysophospholipid receptor G2A activates a specific combination of G proteins and promotes apoptosis. J. Biol. Chem. 278: 14379–14386. [PubMed: 12586833]
4. Le LQ, Kabarowski JH, Weng Z, Satterthwaite AB, Harvill ET, Jensen ER, Miller JF, and Witte ON. 2001 Mice lacking the orphan G protein-coupled receptor G2A develop a late-onset autoimmune syndrome. Immunity 14: 561–571. [PubMed: 11371358]
5. Bolick DT, Skaflen MD, Johnson LE, Kwon SC, Howatt D, Daugherty A, Ravichandran KS, and Hedrick CC. 2009 G2A deficiency in mice promotes macrophage activation and atherosclerosis. Circ. Res. 104: 318–327. [PubMed: 19106413]
6. Parks BW, Gambill GP, Lusis AJ, and Kabarowski JH. 2005 Loss of G2A promotes macrophage accumulation in atherosclerotic lesions of low density lipoprotein receptor-deficient mice. J. Lipid Res. 46: 1405–1415. [PubMed: 15834123]
7. Kabarowski JH 2009 G2A and LPC: regulatory functions in immunity. Prostaglandins Other Lipid Mediat. 89: 73–81. [PubMed: 19383550]
8. Frasch SC, Zemski-Berry K, Murphy RC, Borregaard N, Henson PM, and Bratton DL. 2007 Lysophospholipids of different classes mobilize neutrophil secretory vesicles and induce redundant signaling through G2A. J. Immunol. 178: 6540–6548. [PubMed: 17475884]
9. Chen G, Li J, Qiang X, Czura CJ, Ochani M, Ochani K, Ulloa L, Yang H, Tracey KJ, Wang P, et al. 2005 Suppression of HMGB1 release by stearoyl lysophosphatidylcholine:an additional mechanism for its therapeutic effects in experimental sepsis. J. Lipid Res. 46: 623–627. [PubMed: 15687351]
10. Han KH, Hong KH, Ko J, Rhee KS, Hong MK, Kim JJ, Kim YH, and Park SJ. 2004 Lysophosphatidylcholine up-regulates CXCR4 chemokine receptor expression in human CD4 T cells. J. Leukoc. Biol. 76: 195–202. [PubMed: 15178707]
11. Radu CG, Yang LV, Riedinger M, Au M, and Witte ON. 2004 T cell chemotaxis to lysophosphatidylcholine through the G2A receptor. Proc. Natl. Acad. Sci. USA 101: 245–250. [PubMed: 14681556]
12. Yang LV, Radu CG, Wang L, Riedinger M, and Witte ON. 2005 Gi-independent macrophage chemotaxis to lysophosphatidylcholine via the immunoregulatory GPCR G2A. Blood 105: 1127–1134. [PubMed: 15383458]
13. Yan JJ, Jung JS, Lee JE, Lee J, Huh SO, Kim HS, Jung KC, Cho JY, Nam JS, Suh HW, et al. 2004 Therapeutic effects of lysophos- phatidylcholine in experimental sepsis. Nat. Med. 10: 161–167. [PubMed: 14716308]
14. Wang J, Dotson AL, Murphy SJ, Offner H, and Saugstad JA. 2015 Adoptive transfer of immune subsets prior to MCAO does not exacerbate stroke outcome in splenectomized mice. J. Syst. Integr. Neurosci. 1: 20–28. [PubMed: 26634148]
15. Hong CW, Kim TK, Ham HY, Nam JS, Kim YH, Zheng H, Pang B, Min TK, Jung JS, Lee SN, et al. 2010 Lysophosphatidylcholine increases neutrophil bactericidal activity by enhancement of azurophil granule-phagosome fusion via glycine.GlyR alpha 2/TRPM2/p38 MAPK signaling. J. Immunol. 184: 4401–4413. [PubMed: 20237295]
16. Li PZ, Li JZ, Li M, Gong JP, and He K. 2014 An efficient method to isolate and culture mouse Kupffer cells. Immunol. Lett. 158: 52–56. [PubMed: 24333337]
17. Zhang Y, Geiger JD, and Lautt WW. 1991 Improved high-pressure liquid chromatographic-fluorometric assay for measurement of adenosine in plasma. Am. J. Physiol. 260: G658–G664. [PubMed: 2018140]
18. Wang H, Bloom O, Zhang M, Vishnubhakat JM, Ombrellino M, Che J, Frazier A, Yang H, Ivanova S, Borovikova L, et al. 1999 HMG-1 as a late mediator of endotoxin lethality in mice. Science 285: 248–251. [PubMed: 10398600]
19. Kono H, Fujii H, Ogiku M, Hara M, Tsuchiya M, Ishii K, and Hosomura N. 2012 The Kupffer cell inhibition exacerbates but splenectomy prevents mortality in a rat septic peritonitis model. J. Surg. Res. 175: 101–112. [PubMed: 21492870]
20. Strnad P, Tacke F, Koch A, and Trautwein C. 2017 Liver-guardian, modifier and target of sepsis. Nat. Rev. Gastroenterol. Hepatol. 14: 55–66. [PubMed: 27924081]
21. Koo DJ, Chaudry IH, and Wang P. 1999 Kupffer cells are responsible for producing inflammatory cytokines and hepatocellular dysfunction during early sepsis. J. Surg. Res. 83: 151–157. [PubMed: 10329110]

22. Emmanuilidis K, Weighardt H, Maier S, Gerauer K, Fleischmann T, Zheng XX, Hancock WW, Holzmann B, and Heidecke CD. 2001 Critical role of Kupffer cell-derived IL-10 for host defense in septic peritonitis. J. Immunol. 167: 3919–3927. [PubMed: 11564810]

23. Kawada N, Mizoguchi Y, Kobayashi K, Monna T, Liu P, and Morisawa S. 1992 Enhancement of prostaglandin E2 production by liver macrophages (Kupffer cells) after stimulation with biological response modifiers. Prostaglandins Leukot. Essent. Fatty Acids 46: 105–110. [PubMed: 1502248]

24. Casteleijn E, Kuiper J, Van Rooij HC, Kamps JA, Koster JF, and Van Berkel TJ. 1988 Endotoxin stimulates glycogenolysis in the liver by means of intercellular communication. J. Biol. Chem. 263: 6953–6955. [PubMed: 3284878]

25. Hardonk MJ, Dijkhuis FW, Hulstaert CE, and Koudstaal J. 1992 Heterogeneity of rat liver and spleen macrophages in gadolinium chloride-induced elimination and repopulation. J. Leukoc. Biol. 52: 296–302. [PubMed: 1522388]

26. Lu B, Wang H, Andersson U, and Tracey KJ. 2013 Regulation of HMGB1 release by inflammasomes. Protein Cell 4: 163–167. [PubMed: 23483477]

27. Lu XJ, Chen J, Yu CH, Shi YH, He YQ, Zhang RC, Huang ZA, Lv JN, Zhang S, and Xu L. 2013 LECT2 protects mice against bacterial sepsis by activating macrophages via the CD209a receptor. J. Exp. Med. 210: 5–13. [PubMed: 23254286]

28. Laichalk LL, Kunkel SL, Strieter RM, Danforth JM, Bailie MB, and Standiford TJ. 1996 Tumor necrosis factor mediates lung antibacterial host defense in murine Klebsiella pneumonia. Infect. Immun. 64: 5211–5218. [PubMed: 8945568]

29. Strassmann G, Patil-Koota V, Finkelman F, Fong M, and Kambayashi T. 1994 Evidence for the involvement of interleukin 10 in the differential deactivation of murine peritoneal macrophages by prostaglandin E2. J. Exp. Med. 180: 2365–2370. [PubMed: 7525853]

30. Murakami N, Hashidate T, Harayama T, Yokomizo T, Shimizu T, and Nakamura M. 2009 Transcriptional regulation of human G2A in mono-cytes/ macrophages: involvement of c/EBPs, Runx and Pu.1. Genes Cells 14: 1441–1455. [PubMed: 19930466]

31. Ward PA 2008 Sepsis, apoptosis and complement. Biochem. Pharmacol. 76: 1383–1388. [PubMed: 18848819]

32. Peters-Golden M 2009 Putting on the brakes: cyclic AMP as a multipronged controller of macrophage function. Sci. Signal. 2: pe37. [PubMed: 19531801]

33. Haskó G, Németh ZH, Szabó C, Zsilla G, Salzman AL, and Vizi ES. Isoproterenol inhibits Il-10, TNF-alpha, and nitric oxide production in RAW 264.7 macrophages. Brain Res. Bull. 45: 183–187. [PubMed: 9443838]

34. Gerold M, Cavero I, Riggenbach H, Wall M, and Haeusler G. 1976 Analysis of cardiac chronotropic responses to diazepam and bromazepam in conscious trained dogs. Eur. J. Pharmacol. 35: 361–368. [PubMed: 2483]

35. Muthu K, He LK, Szilagyi A, Strotmon P, Gamelli RL, and Shankar R. 2010 ß-adrenergic stimulation increases macrophage CD14 expression and E coli phagocytosis through PKA signaling mechanisms. J. Leukoc. Biol. 88: 715–724. [PubMed: 20643814]

36. Lynge J, Schulte G, Nordsborg N, Fredholm BB, and Hellsten Y. 2003 Adenosine A 2B receptors modulate cAMP levels and induce CREB but not ERK1/2 and p38 phosphorylation in rat skeletal muscle cells. Biochem. Biophys. Res. Commun. 307: 180–187. [PubMed: 12849998]

37. Xaus J, Mirabet M, Lloberas J, Soler C, Lluis C, Franco R, and Celada A.1999 IFN-gamma up-regulates the A2B adenosine receptor expression in macrophages: a mechanism of macrophage deactivation. J. Immunol. 162: 3607–3614. [PubMed: 10092821]

38. Streitova D, Hofer M, Hola J, Vacek A, and Pospisil M. 2010 Adenosine A (1), A(2a), A(2b), and A(3) receptors in hematopoiesis. 2. Expression of receptor mRNA in resting and lipopolysaccharide-activated mouse RAW 264.7 macro-phages. Physiol. Res. 59: 139–144. [PubMed: 19249906]

39. Sousa LP, Lopes F, Silva DM, Tavares LP, Vieira AT, Rezende BM, Carmo AF, Russo RC, Garcia CC, Bonjardim CA, et al. 2010 PDE4 inhibition drives resolution of neutrophilic inflammation by inducing apoptosis in a PKA-PI3K/Akt-dependent and NF-kappaB-independent manner. J. Leukoc. Biol. 87: 895–904. [PubMed: 20103769]

40. Krajcovic M, Krishna S, Akkari L, Joyce JA, and Overholtzer M. 2013 mTOR regulates phagosome and entotic vacuole fission. Mol. Biol. Cell 24: 3736–3745. [PubMed: 24088573]
41. Edwards MW, Aultman JA, Harber G, Bhatt JM, Sztul E, Xu Q, Zhang P, Michalek SM, and Katz J. 2013 Role of mTOR downstream effector signaling molecules in Francisella tularensis internalization by murine macrophages. PLoS One 8: e83226.
42. Traeger T, Mikulcak M, Eipel C, Abshagen K, Diedrich S, Heidecke CD, Maier S, and Vollmar B. 2010 Kupffer cell depletion reduces hepatic inflammation and apoptosis but decreases survival in abdominal sepsis. Eur. J. Gastroenterol. Hepatol. 22: 1039–1049. [PubMed: 20300005]
43. Dahle MK, øverland G, Myhre AE, Stuestøl JF, Hartung T, Krohn CD, Mathiesen ø., Wang JE, and Aasen AO. 2004 The phosphatidylinositol 3-kinase/protein kinase B signaling pathway is activated by lipoteichoic acid and plays a role in Kupffer cell production of interleukin-6 (IL-6) and IL-10. Infect. Immun. 72: 5704–5711. [PubMed: 15385469]
44. Mosmann TR 1994 Properties and functions of interleukin-10. Adv. Immunol. 56: 1–26. [PubMed: 8073945]
45. Husztik E, Lázár G, and Párducz A. 1980 Electron microscopic study of Kupffer-cell phagocytosis blockade induced by gadolinium chloride. Br. J. Exp. Pathol. 61: 624–630. [PubMed: 7459256]
46. Dieter P, Schulze-Specking A, and Decker K. 1988 Ca2+ requirement of prostanoid but not of superoxide production by rat Kupffer cells. Eur. J. Bio- chem. 177: 61–67.
47. Urade Y, Ujihara M, Horiguchi Y, Ikai K, and Hayaishi O. 1989 The major source of endogenous prostaglandin D2 production is likely antigen-presenting cells. Localization of glutathione-requiring prostaglandin D synthetase in histiocytes, dendritic, and Kupffer cells in various rat tissues. J. Immunol. 143: 2982–2989. [PubMed: 2509561]
48. MacKenzie KF, Clark K, Naqvi S, McGuire VA, Nöehren G, Kristariyanto Y, van den Bosch M, Mudaliar M, McCarthy PC, Pattison MJ, et al. 2013 PGE(2) induces macrophage IL-10 production and a regulatory-like phenotype via a protein kinase A-SIK-CRTC3 pathway. J. Immunol. 190: 565–577. [PubMed: 23241891]
49. Murata T, Aritake K, Tsubosaka Y, Maruyama T, Nakagawa T, Hori M, Hirai H, Nakamura M, Narumiya S, Urade Y, and Ozaki H. 2013 Anti-inflammatory role of PGD2 in acute lung inflammation and therapeutic application of its signal enhancement. Proc. Natl. Acad. Sci. USA 110: 5205–5210. [PubMed: 23479612]
50. Seow V, Lim J, Iyer A, Suen JY, Ariffin JK, Hohenhaus DM, Sweet MJ, and Fairlie DP. 2013 Inflammatory responses induced by lipopolysaccharide are amplified in primary human monocytes but suppressed in macrophages by complement protein C5a. J. Immunol. 191: 4308–4316. [PubMed: 24043889]
51. Bourne HR, Lichtenstein LM, Melmon KL, Henney CS, Weinstein Y, and Shearer GM. 1974 Modulation of inflammation and immunity by cyclic AMP. Science 184: 19–28. [PubMed: 4131281]
52. Wall EA, Zavzavadjian JR, Chang MS, Randhawa B, Zhu X, Hsueh RC, Liu J, Driver A, Bao XR, Sternweis PC, et al. 2009 Suppression of LPS-induced TNF-alpha production in macrophages by cAMP is mediated by PKA-AKAP95-p105. Sci. Signal. 2: ra28. [PubMed: 19531803]
53. Yan Y, Jiang W, Liu L, Wang X, Ding C, Tian Z, and Zhou R. 2015 Dopamine controls systemic inflammation through inhibition of NLRP3 inflam- masome. Cell 160: 62–73. [PubMed: 25594175]
54. Lee GS, Subramanian N, Kim AI, Aksentijevich I, Goldbach-Mansky R, Sacks DB, Germain RN, Kastner DL, and Chae JJ. 2012 The calcium- sensing receptor regulates the NLRP3 inflammasome through Ca2+ and cAMP. Nature 492: 123–127. [PubMed: 23143333]
55. Neméth ZH, Lutz CS, Csóka B, Deitch EA, Leibovich SJ, Gause WC, Tone M, Pacher P, Vizi ES, and Hasko G. 2005 Adenosine augments IL-10 production by macrophages through an A2B receptor-mediated posttranscriptional mechanism. J. Immunol. 175: 8260–8270. [PubMed: 16339566]
56. Haskó G, Csóka B, Nemeth ZH, Vizi ES, and Pacher P. 2009 A(2B) adenosine receptors in immunity and inflammation. Trends Immunol. 30: 263–270. [PubMed: 19427267]

57. Csóka B, Selmeczy Z, Koscsó B, Németh ZH, Pacher P, Murray PJ, Kepka-Lenhart D, Morris SM Jr., Gause WC, Leibovich SJ, and Haskó G. 2012 Adenosine promotes alternative macrophage activation via A2A and A2B receptors. FASEB J. 26: 376–386. [PubMed: 21926236]
58. Csóka B, Koscsó B, Töro G, Kókai E, Virág L, Németh ZH, Pacher P, Bai P, and Hasko G. 2014 A2B adenosine receptors prevent insulin resistance by inhibiting adipose tissue inflammation via maintaining alternative macro-phage activation. Diabetes 63: 850–866. [PubMed: 24194503]
59. Koscsó B, Csoka B, Kókai E, Nemeth ZH, Pacher P, Virág L, Leibovich SJ, and Haskó G. 2013 Adenosine augments IL-10-induced STAT3 signaling in M2c macrophages. J. Leukoc. Biol. 94: 1309–1315. [PubMed: 23922379]
60. Csóka B, Németh ZH, Rosenberger P, Eltzschig HK, Spolarics Z, Pacher P, Selmeczy Z, Koscso B, Himer L, Vizi ES, et al. 2010 A2B adenosine receptors protect against sepsis-induced mortality by dampening excessive inflammation. J. Immunol. 185: 542–550. [PubMed: 20505145]
61. Hinz S, Navarro G, Borroto-Escuela D, Seibt BF, Ammon YC, de Filippo E, Danish A, Lacher SK, Červinková B, Rafehi M, et al. 2018 Adenosine A2A receptor ligand recognition and signaling is blocked by A2A receptors. Oncotarget 9: 13593–13611. [PubMed: 29568380]
62. Vogel SN, Weedon LL, Oppenheim JJ, and Rosenstreich DL. 1981 Defective Fc-mediated phagocytosis in C3H/HeJ macrophages. II. Correction by cAMP agonists. J. Immunol. 126: 441–45. [PubMed: 6256439]
63. Sousa LP, Carmo AF, Rezende BM, Lopes F, Silva DM, Alessandri AL, Bonjardim CA, Rossi AG, Teixeira MM, and Pinho V. 2009 Cyclic AMP enhances resolution of allergic pleurisy by promoting inflammatory cell apoptosis via inhibition of PI3K/Akt and NF-kappaB. Biochem. Pharmacol. 78: 396–405. [PubMed: 19422809]
64. Moore AR, and Willoughby DA. 1995 The role of cAMP regulation in controlling inflammation. Clin. Exp. Immunol. 101: 387–389. [PubMed: 7664483]
65. Bystrom J, Evans I, Newson J, Stables M, Toor I, van Rooijen N, Crawford M, Colville-Nash P, Farrow S, and Gilroy DW. 2008 Resolution-phase macrophages possess a unique inflammatory phenotype that is controlled by cAMP. Blood 112: 4117–127. [PubMed: 18779392]
66. Song G, Ouyang G, and Bao S. 2005 The activation of Akt/PKB signaling pathway and cell survival. J. Cell. Mol Med. 9: 59–71. [PubMed: 15784165]
67. Hong K, Lou L, Gupta S, Ribeiro-Neto F, and Altschuler DL. 2008 A novel Epac-Rap-PP2A signaling module controls cAMP-dependent Akt regulation. J. Biol. Chem. 283: 23129–23138. [PubMed: 18550542]
68. Kim S, Jee K, Kim D, Koh H, and Chung J. 2001 Cyclic AMP inhibits Akt activity by blocking the membrane localization of PDK1. J. Biol. Chem. 276: 12864–12870. [PubMed: 11278269]
69. Makhov P, Golovine K, Teper E, Kutikov A, Mehrazin R, Corcoran A, Tulin A, Uzzo RG, and Kolenko VM. 2014 Piperlongumine promotes autophagy via inhibition of Akt/mTOR signalling and mediates cancer cell death. Br. J. Cancer 110: 899–907. [PubMed: 24434432]
70. Crowell B, Lee GH, Nikolaeva I, Dal Pozzo V, and D'Arcangelo G. 2015 Complex neurological phenotype in mutant mice lacking Tsc2 in excitatory neurons of the developing Forebrain(123). eNeuro. DOI: 10.1523/ENEUR0.0046-15.2015.
71. Byles V, Covarrubias AJ, Ben-Sahra I, Lamming DW, Sabatini DM, Manning D, and Horng T. 2013 The TSC-mTOR pathway regulates macrophage polarization. Nat. Commun. 4: 2834. [PubMed: 24280772]
72. Leclerc GM, Leclerc GJ, Fu G, and Barredo JC. 2010 AMPK-induced activation of Akt by AICAR is mediated by IGF-1R dependent and independent mechanisms in acute lymphoblastic leukemia. J. Mol. Signal. 5: 15. [PubMed: 20863384]
73. Shiratsuchi H, and Basson MD. 2007 Akt2, but not Akt1 or Akt3 mediates pressure-stimulated serum-opsonized latex bead phagocytosis through activating mTOR and p70 S6 kinase. J. Cell. Biochem. 102: 353–367. [PubMed: 17372934]
74. Thomson AW, Turnquist HR, and Raimondi G. 2009 Immunoregulatory functions of mTOR inhibition. Nat. Rev. Immunol. 9: 324–337. [PubMed: 19390566]
75. Bolick DT, Whetzel AM, Skaflen M, Deem TL, Lee J, and Hedrick CC. 2007 Absence of the G protein-coupled receptor G2A in mice promotes monocyte/endothelial interactions in aorta. Circ. Res. 100: 572–580. [PubMed: 17255525]

76. Parks BW, Lusis AJ, and Kabarowski JH. 2006 Loss of the lyso-phosphatidylcholine effector, G2A, ameliorates aortic atherosclerosis in low-density lipoprotein receptor knockout mice. Arterioscler. Thromb. Vasc. Biol. 26: 2703–2709. [PubMed: 16990555]

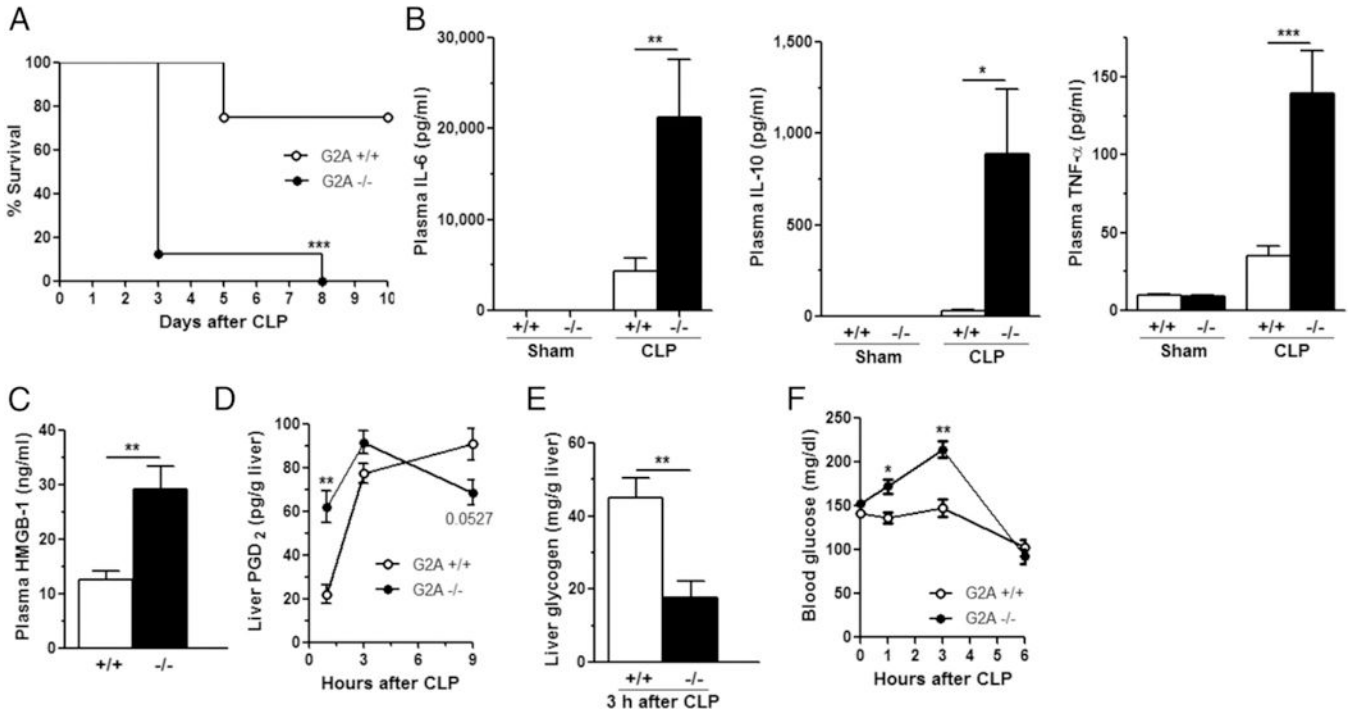

FIGURE 1.

Enhanced susceptibility to sepsis in G2A$^{-/-}$ mice. (**A**) Survival of G2A$^{+/+}$ and G2A$^{-/-}$ mice after CLP (one-puncture model; $n = 8$). (**B**) Plasma cytokine levels in G2A$^{+/+}$ and G2A$^{-/-}$ mice at 8 h after CLP ($n = 8$–17). (**C**) Plasma HMGB-1 levels in G2A$^{+/+}$ and G2A$^{-/-}$ mice at 24 h after CLP ($n = 7$). (**D**) PGD_2 level in liver at 1, 3, and 9 h post-CLP ($n = 4$). (**E**) Glycogen level in liver at 3 h post-CLP ($n = 5$). (**F**) Blood glucose level up to 6 h after CLP ($n = 49$–52) (for zero time point) and 8–10 (for other time points). Animal survival was analyzed by log-rank (Mantel–Cox) test in (A), one-way ANOVA and post hoc Bonferroni test were used in (B)–(D), and t test was used in (E) and (F). *p <0.05, **p <0.01, ***p <0.001.

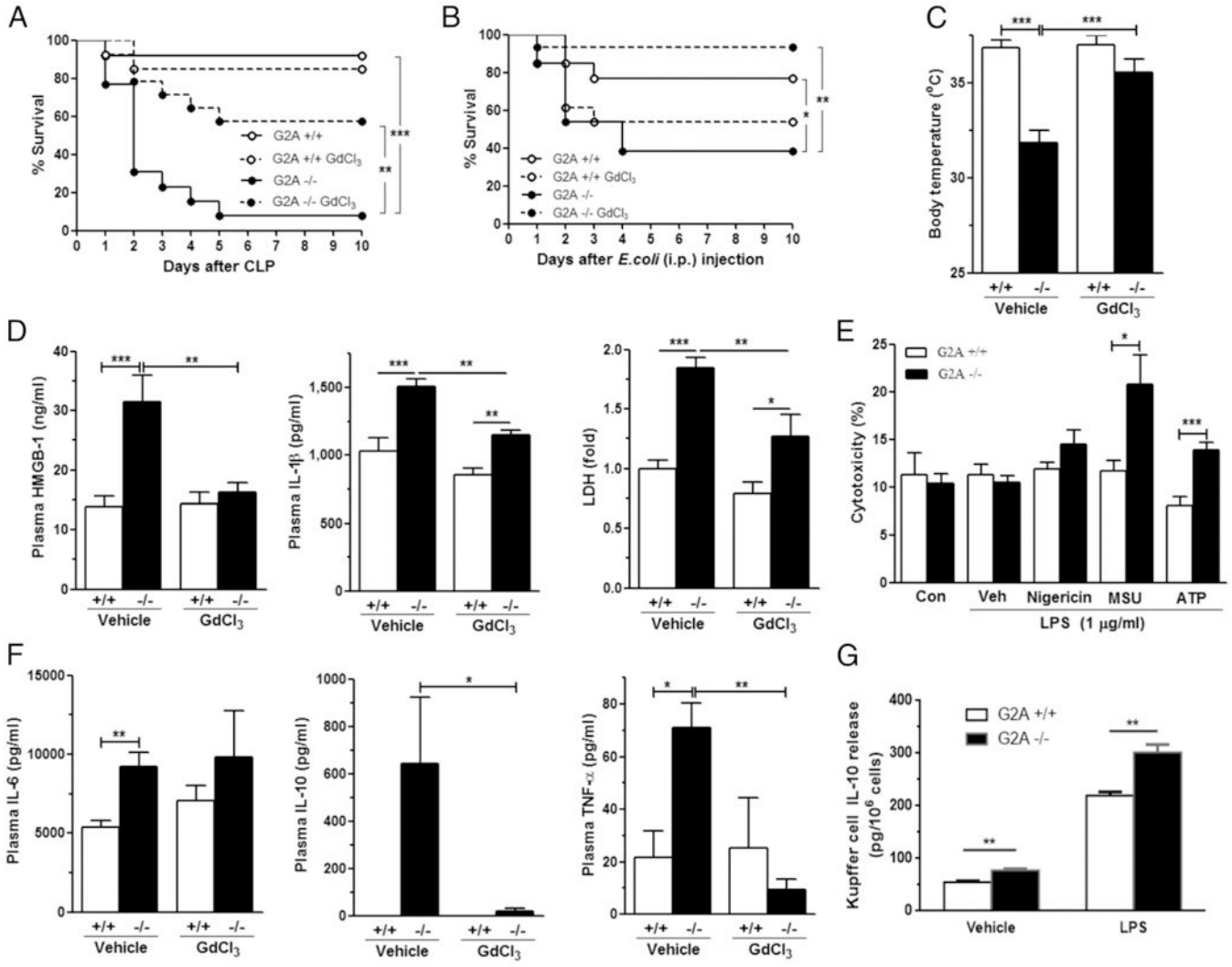

FIGURE 2.

$GdCl_3$ rescues $G2A^{-/-}$ mice from enhanced susceptibility to sepsis and blocks various exaggerated responses to CLP. (**A**) Survival after CLP in the saline- or $GdCl_3$-pretreated $G2A^{+/+}$ and $G2A^{-/-}$ mice (n =11–14). (**B**) Survival after *E.* coli-induced sepsis in the saline- or $GdCl_3$-pretreated $G2A^{+/+}$ and $G2A^{-/-}$ mice (n = 13–15). (**C**) Rectal temperature at 24 h after CLP in the saline- or $GdCl_3$-treated $G2A^{+/+}$ and $G2A^{-/-}$ mice (n = 8–11). (**D** and **F**) Post-CLP plasma levels of HMGB-1, IL-1β, LDH, IL-6, IL-10, and TNF-α in the saline- or $GdCl_3$-pretreated $G2A^{+/+}$and $G2A^{-/-}$ mice (n = 4–11). (**E**) NLRP3 inflammasome responses in isolated Kupffer cells from $G2A^{-/-}$, but not $G2A^{+/+}$, mice (n = 8–9). (**G**) Both basal and LPS-stimulated IL-10 release from Kupffer cells isolated from $G2A^{+/+}$ and $G2A^{-/-}$ mice measured at 8 h after the addition of LPS (1 μg/ml). A t test was used in (A), (B), and (E), and one-way ANOVA and post hoc Bonferroni test were used in (C), (D), and (F). *$p < 0.05$, **$p < 0.01$, ***$p < 0.001$.

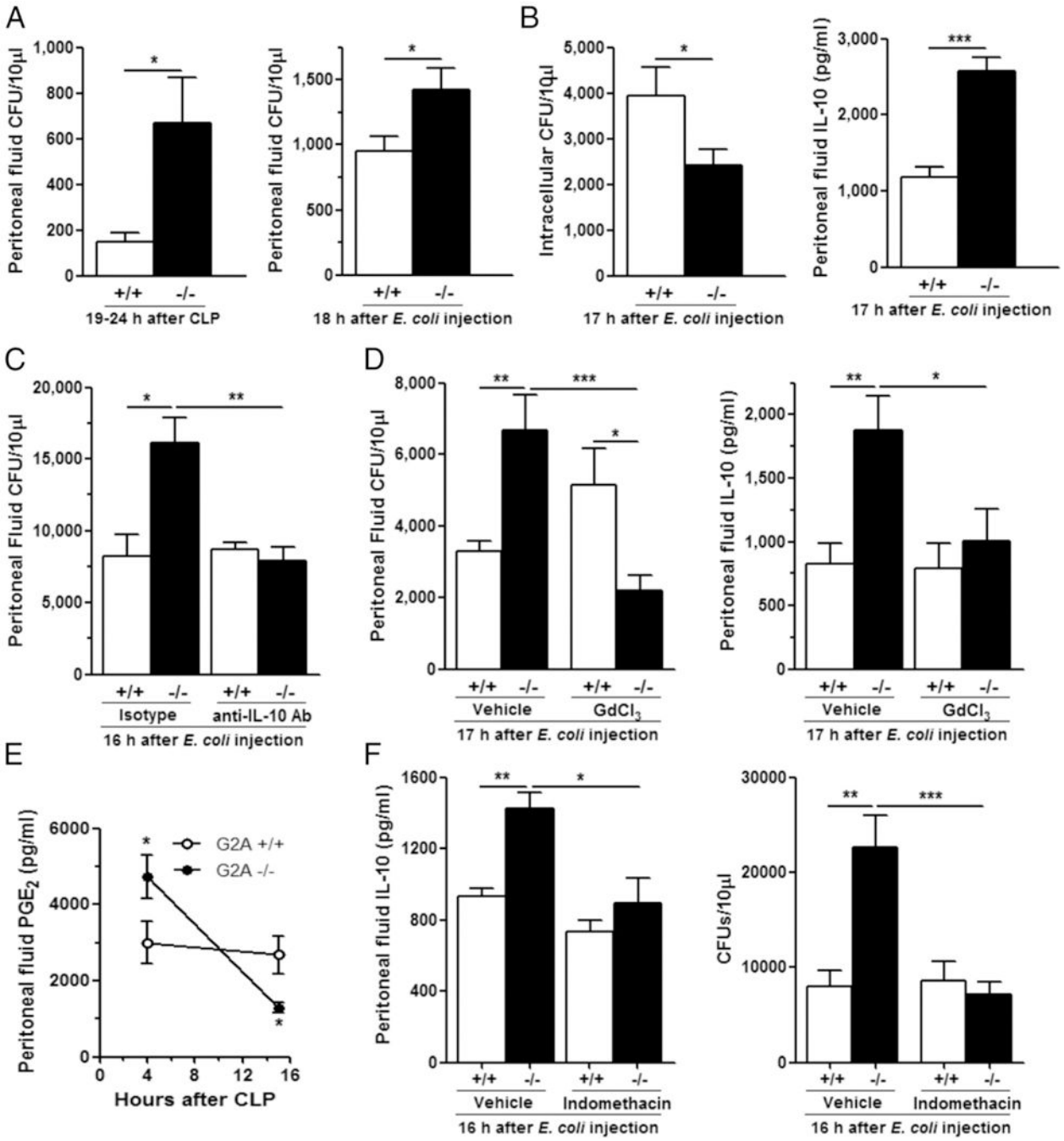

FIGURE 3.

Increases in peritoneal viable bacteria and IL-10 level in G2A$^{-/-}$ mice. (**A**) Number of viable bacteria in the peritoneal lavage fluid at 19–24 h after CLP and at 18 h after E. coli injection (n = 7–13). (**B**) Number of viable bacteria in the peritoneal exudates cells at 17 h after *E. coli* injection and peritoneal lavage fluid IL-10 level from G2A$^{+/+}$ and G2A$^{-/-}$ mice at 17 h after *E. coli* injection (n = 9–10). (**C**) Number of viable bacteria in the peritoneal lavage fluid at 16 h after *E. coli* injection in the isotype– or anti–IL-10 Ab-pretreated G2A$^{+/+}$ and G2A$^{-/-}$ mice (n = 5). (**D**) Number of viable bacteria and IL-10 level in the peritoneal

lavage fluid at 17 h after *E. coli* injection in the saline- or $GdCl_3$-pretreated $G2A^{+/+}$ and $G2A^{-/-}$ mice (n = 10–12). (**E**) Peritoneal lavage fluid PGE_2 level from $G2A^{+/+}$ and $G2A^{-/-}$ mice at 4 and 15 h after CLP (n = 8–12). (**F**) IL-10 level and the number of viable bacteria in the peritoneal lavage fluid from $G2A^{+/+}$ and $G2A^{-/-}$ in the saline- or indomethacin-pretreated mice at 16 h after E. *coli* injection (n = 8–9). Indomethacin (5 mg/kg, i.p.) was injected 1 h before *E. coli* injection. A t test was used in (A), (B), and (E), and one-way ANOVA and post hoc Bonferroni test were used in (C), (D), and (F). *$p < 0.05$, **$p < 0.01$, ***$p < 0.001$.

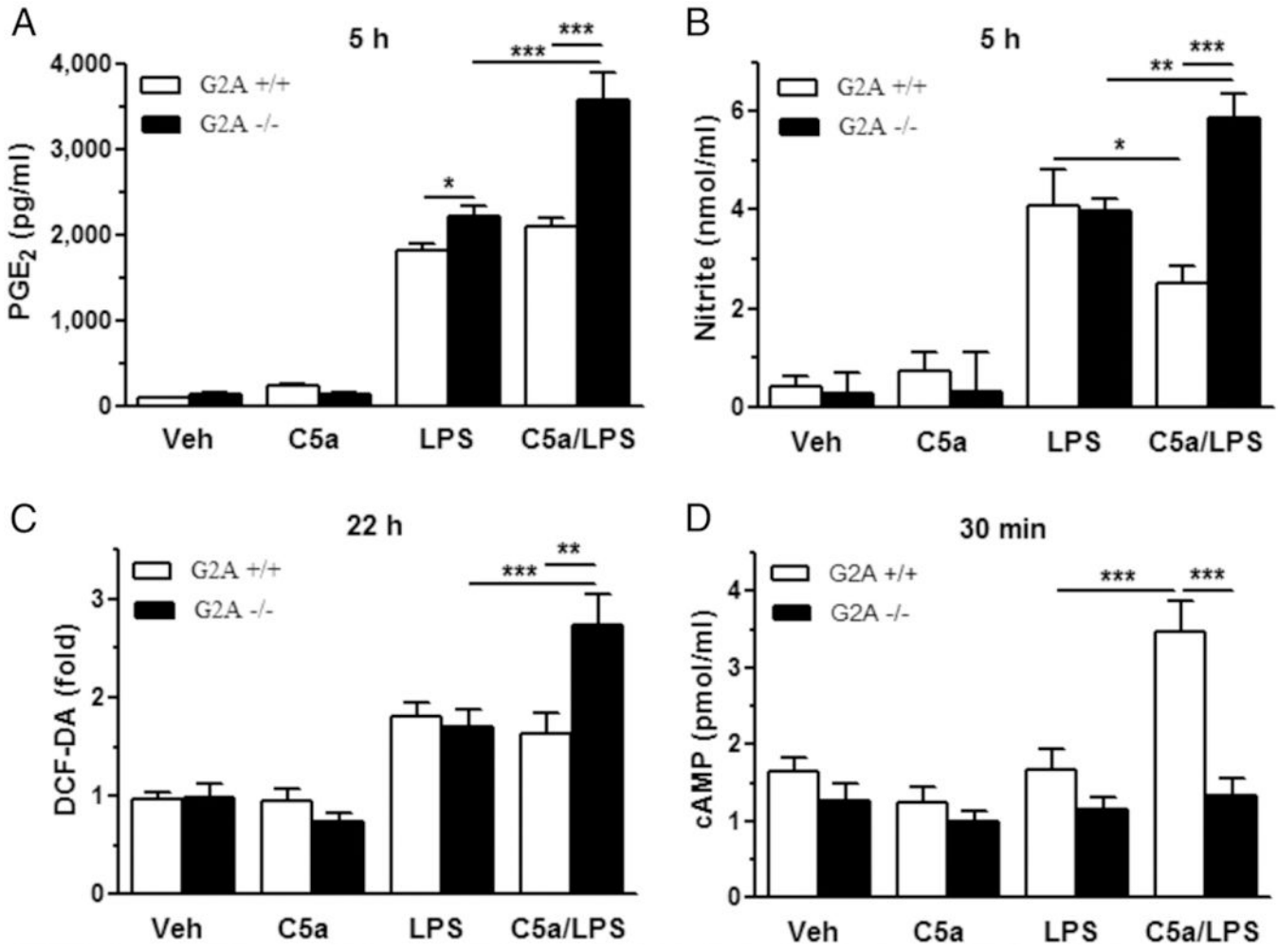

FIGURE 4.

Aberrant responses of $G2A^{-/-}$ macrophages to the in vitro condition of sepsis. Levels of PGE_2 (**A**) and nitrite (**B**) in the medium were measured at 5 h after stimulation with C5a (1 μg/ml), LPS (1 μg/ml), or both ($n = 8–9$). (**C**) Intracellular ROS generation was measured using DCF-DA at 22 h after stimulation with C5a, LPS, or both ($n = 12–14$). (**D**) Intracellular cAMP levels were measured at 30 min after stimulation with C5a, LPS, or both ($n = 6–9$). One-way ANOVA and post hoc Bonferroni test were used. *$p < 0.05$, **$p < 0.01$, ***$p < 0.001$.

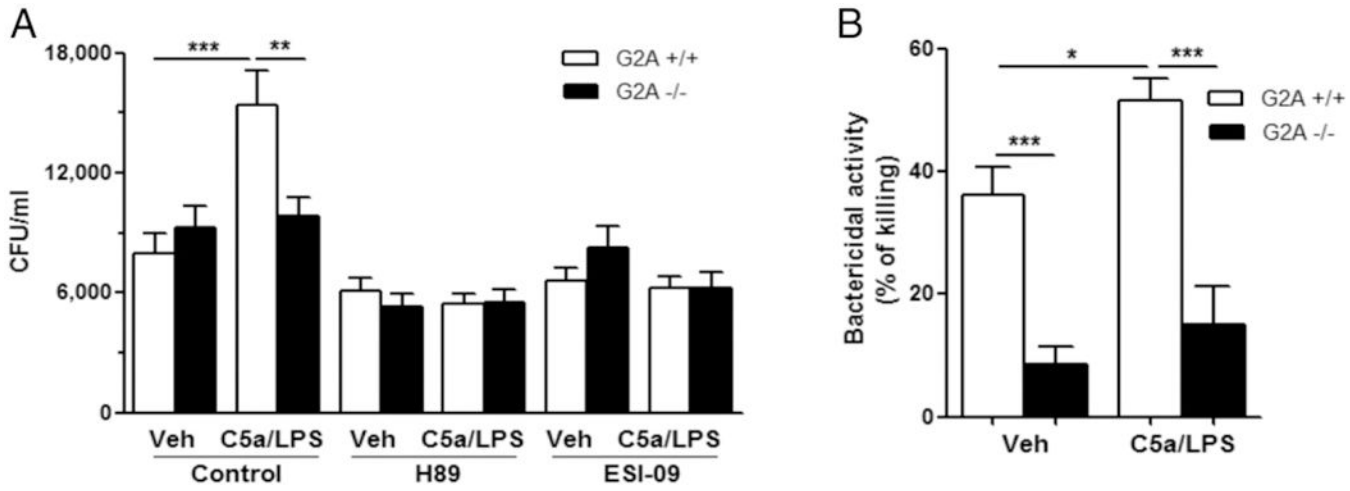

FIGURE 5.

C5a/LPS stimulation increases phagocytosis in $G2A^{+/+}$, but not $G2A^{-/-}$, macrophages via cAMP signaling. (**A**) Thioglycolate-induced macrophages were costimulated with C5a/LPS for 5 h, and then *E. coli* phagocytosis was determined (n = 9–21). PKA inhibitor (H-89, 10 μM) or EPAC inhibitor (ESI-09, 10 μM) was applied just before the addition of C5a/LPS (n = 9–12). (**B**) Thioglycolate-induced macrophages were costimulated with C5a/LPS for 5 h, and then *E. coli* bactericidal activity was determined (n = 8–9). One-way ANOVA and post hoc Bonferroni test were used. *p < 0.05, **p<, 0.01, ***p< 0.001.

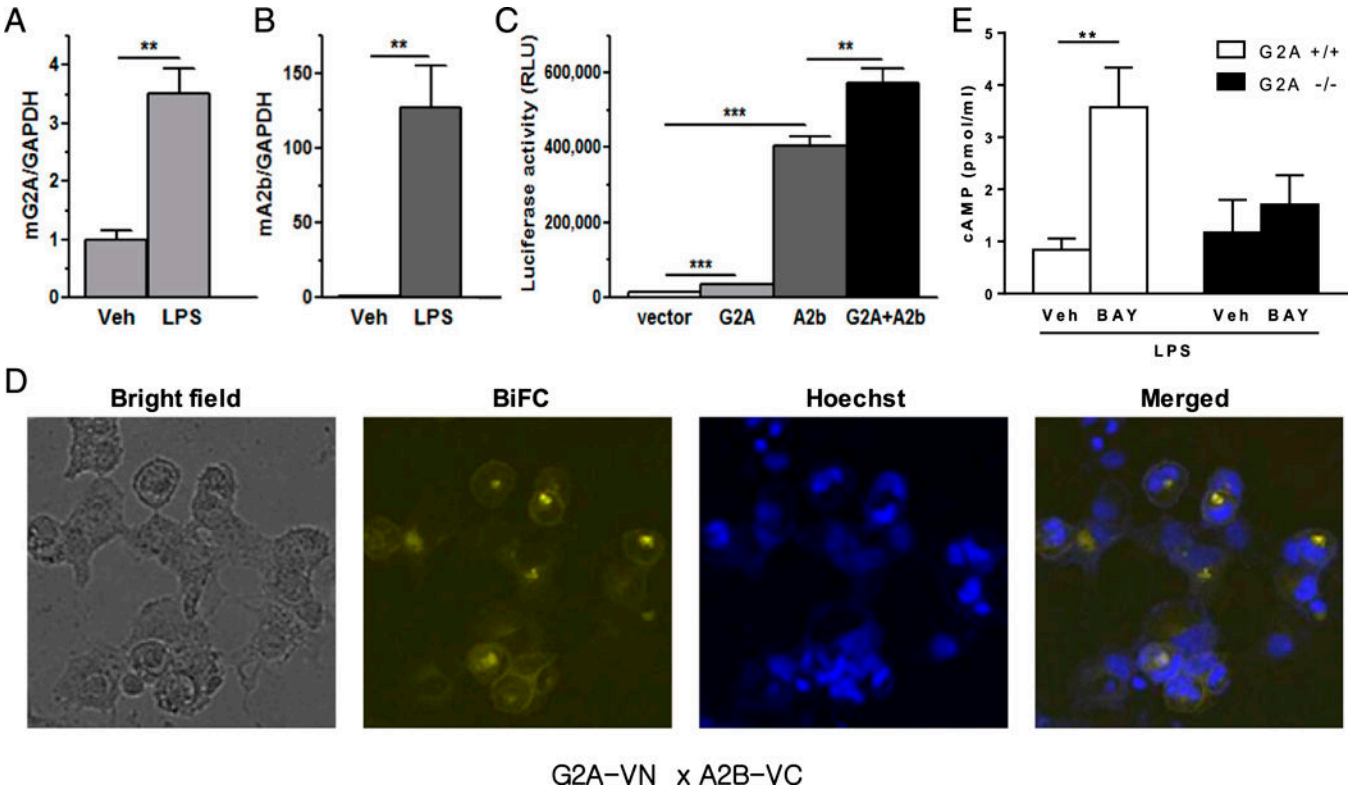

FIGURE 6.

Evidence suggesting cooperativity between G2A and A2bR in cAMP signaling. (**A** and **B**) mRNA levels of G2A and A2bAR in thioglycolate-induced peritoneal macrophages at 5 h after LPS (1 mg/ml) stimulation ($n = 3$). (**C**) HEK-293 cells were transfected for 24 h with empty vector + cAMP-luc, G2A + cAMP-luc, A2bAR + cAMP-luc, and G2A + A2bAR + cAMP-luc reporter plasmids, and then luciferase activity was measured in cell lysates. These data represent three independent experiments. (**D**) BiFC analysis of physical interaction between G2A and A2bAR. Original magnification ×200. (**E**) After the preincubation with LPS (1 μg/ml) for 24 h, the isolated Kupffer cells from $G2A^{+/+}$ and $G2A^{-/-}$ mice were incubated with BAY 60–6583 (1 μM), a specific agonist for A2bAR, for 10 min, and the intracellular cAMP levels were measured. *t* test was used. $^{**}p < 0.01$, $^{***}p < 0.001$.

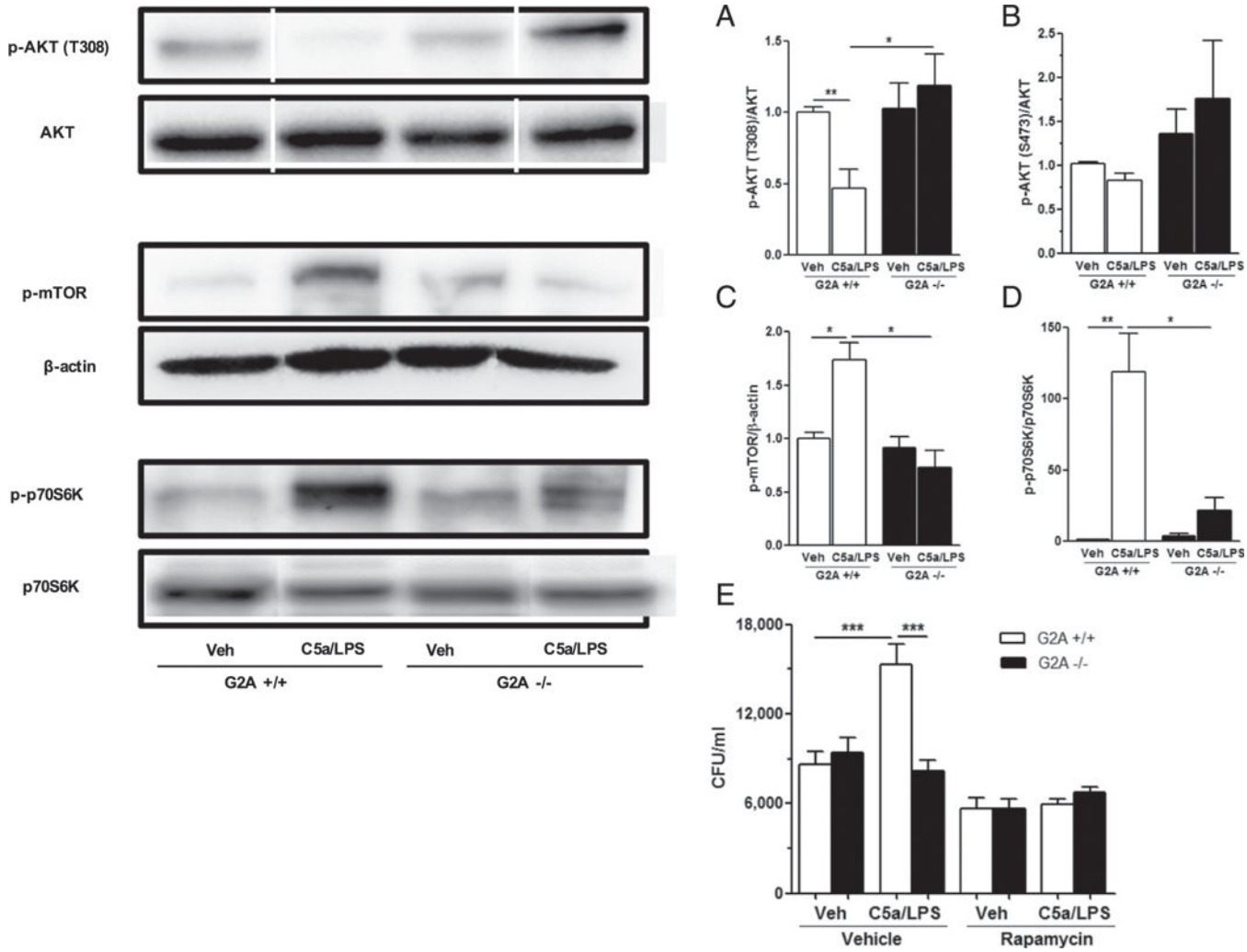

FIGURE 7.

C5a/LPS stimulation induces differential intracellular signaling in $G2A^{+/+}$ and $G2A^{-/-}$ macrophages. Thioglycolate-induced macro-phages were costimulated with C5a/LPS for 30 min, and then cell lysates were harvested. (**A–D**) Western blot analysis was performed using Akt, phospho-Akt, phospho-mTOR, p70S6K, and phospho-p70S6K Abs ($n = 3–5$). The white lines indicate where parts of the image were joined. (**E**) Thioglycolate-induced macrophages were costimulated with C5a/LPS for 5 h, and then *E. coli* phagocytosis was determined. An mTOR inhibitor (rapamycin, 100 nM) was applied before the addition of C5a/LPS ($n = 9$). A *t* test was used in (A)–(D), and one-way ANOVA and post hoc Bonferroni test were used in (E). $*p < 0.05$, $**p < 0.01$, $***p < 0.001$.

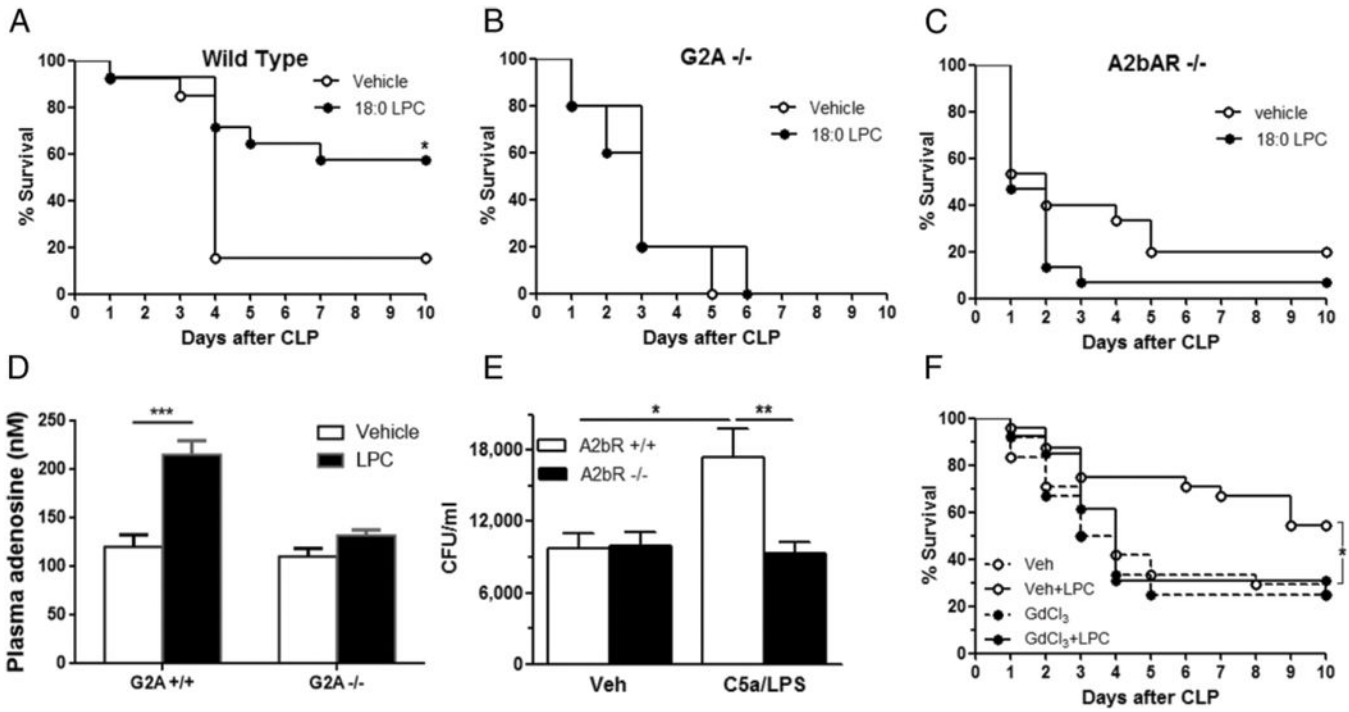

FIGURE 8.

LPC has no protective effect on CLP-induced sepsis in either $G2A^{-/-}$ or $A2bAR^{-/-}$ mice and in $GdCl_3$-pretreated mice. Mice were injected s.c. with vehicle (saline containing 2% BSA) or LPC (10 mg/kg) four times at 12-h intervals beginning 2 h after CLP (**A–C** and **F**). (A–C) Survival of wild-type mice, $G2A^{-/-}$ mice, and $A2aAR^{-/-}$ mice after CLP ($n = 6–14$). (**D**) Plasma adenosine levels in $G2A^{+/+}$ and $G2A^{-/-}$ mice at 1 h after LPC injection (10 mg/kg, s.c.) ($n = 5–10$). (E) $A2bAR^{-/-}$ thioglycolate-induced macrophages were costimulated with C5a/LPS for 5 h, and then *E. coli* phagocytosis was determined ($n = 11–12$). (F) ICR mice were pretreated with $GdCl_3$ (20 mg/kg) via tail vein at 24 h prior to CLP ($n = 12–24$). Animal survival was analyzed by log-rank (Mantel–Cox) test in (A)–(C) and (F), and one-way ANOVA and post hoc Bonferroni test were used in (D) and (E). $*p < 0.05$, $**p < 0.01$, $***p < 0.001$.